Microbiology (2009), **155**, 3922–3933 DOI 10.1099/mic.0.030825-0

Deletion of Mid1, a putative stretch-activated calcium channel in *Claviceps purpurea*, affects vegetative growth, cell wall synthesis and virulence

Jörg Bormann and Paul Tudzynski

Institut für Botanik, Westfälische Wilhelms-Universität Münster, Schloßgarten 3, D-48149 Münster, Germany

Correspondence
Paul Tudzynski
tudzyns@uni-muenster.de

Received 13 May 2009
Revised 14 September 2009
Accepted 15 September 2009

The putative *Claviceps purpurea* homologue of the *Saccharomyces cerevisiae* stretch-activated calcium ion channel Mid1 was investigated for its role in vegetative growth, differentiation and pathogenicity on rye (*Secale cereale*). Gene replacement mutants of *Cl. purpurea mid1* were not affected in polar growth and branching in axenic culture but showed a significantly reduced growth rate. The growth defect could not be complemented by Ca^{2+} supplementation, in contrast to *mid1* mutants in yeast, but the altered sensitivity of the mutants to changes in external and internal Ca^{2+} concentrations indicates some role of Mid1 in Ca^{2+} homeostasis. The major effect of *mid1* deletion, however, was the complete loss of virulence: infected rye plants showed no disease symptoms at all. Detailed analyses of *in vitro*-infected rye ovaries demonstrated that the Δ*mid1* mutants had multiple apical branches and were unable to infect the host tissue, suggesting that Mid1 is essential for generating the necessary mechanical force for penetration. This is believed to be the first report of an essential role for a Mid1 homologue in the virulence of a plant-pathogenic fungus.

INTRODUCTION

The phytopathogenic biotrophic ascomycete *Claviceps purpurea* (Fries ex Fries) Tulasne parasitizes a large number of Poaceae species (Tudzynski & Scheffer, 2004). It colonizes ovaries of its main host, rye (*Secale cereale*), by penetrating the cuticle and growing through the ovarian tissue in a strictly directed and unbranched manner until it reaches the vascular bundles. By tapping into the vascular bundles, the fungus assures a stable nutrition supply. This is a prerequisite for the subsequent colonization of the entire ovary. During this process the fungus produces masses of conidia which are secreted in a viscous fluid called honeydew. Spores are dispersed to other blooming florets mainly zoochorically and hydrochorically. The period of conidia formation ends when sclerotium formation is initiated. The sclerotia represent resting structures consisting of a solid plectenchymatous structure of pigmented storage cells (Tenberge, 1999). They contain the so-called ergot alkaloids, which represent a class of pharmacologically important mycotoxins (Schardl *et al.*, 2006).

Abbreviations: CW calcofluor white; FITC-WGA, fluorescein isothiocyanate-labelled wheatgerm agglutinin.

The GenBank/EMBL/DDBJ accession number for the *mid1* gene of *Claviceps purpurea* is FM945328.

Five supplementary figures are available with the online version of this paper.

The fungus grows mainly intercellularly and therefore decomposes the middle lamella between the plant cells. This lamella predominantly consists of pectin; degradation of pectin by fungal polygalacturonases is essential for full pathogenicity (Oeser *et al.*, 2002). It is possible that Ca^{2+} complexed in this pectin could act as a trail for the hyphae on their way through the ovary. A tip-high gradient of cytoplasmic calcium ($[Ca^{2+}]_{cyt.}$) has been observed in a wide range of eukaryotes that grow in a polarized and oriented manner, including fungal hyphae (Jackson & Heath, 1993; Silverman-Gavrila & Lew, 2003), neurons (Mattson, 1999), and pollen tubes and root hairs of vascular plants (Hepler *et al.*, 2001; Malhó & Trewavas, 1996; Pierson *et al.*, 1994); *Cl. purpurea* may possess a similar gradient. Ca^{2+} is one of the main signal mediators in eukaryotic cells and regulates a wide range of cellular processes such as gene expression (Yoshimoto *et al.*, 2002) and cytoskeleton rearrangements (Torralba & Heath, 2001), e.g in response to external stimuli and stresses (Cyert, 2003; Kraus & Heitman, 2003).

One of the key players in Ca^{2+} homeostasis and generation of $[Ca^{2+}]_{cyt.}$ gradients is the Ca^{2+}-permeable, stretch-activated nonselective cation channel Mid1. It seems to mediate Ca^{2+} uptake as a result of membrane distension, as shown in several polar-growing organisms, including *Saprolegnia ferax* (Garrill *et al.*, 1993) and *Candida albicans* (Watts *et al.*, 1998), and in roots of *Arabidopsis thaliana* (Nakagawa *et al.*, 2007).

Downloaded from www.sgmjournals.org by
IP: 93.91.26.109
On: Wed, 02 Sep 2015 10:32:12
030825 © 2009 SGM Printed in Great Britain

The role of Mid1 in different organisms is highly variable. While in yeast Mid1 is essential for viability upon response to mating pheromone (Iida *et al.*, 1994), it has no impact on mating in *Neurospora crassa* (Lew *et al.*, 2008). The tip-high Ca^{2+} gradient necessary for polar growth (Jackson & Heath, 1993; Silverman-Gavrila & Lew, 2003) is obviously generated in different ways: in *S. ferax* tip-localized Ca^{2+} channels establish and maintain the gradient (Garrill *et al.*, 1993), whereas in *N. crassa* the Ca^{2+} originates mainly from intracellular storage compartments (Levina *et al.*, 1995; Silverman-Gavrila & Lew, 2002). In the latter case it is proposed that Mid1 mainly plays a role in Ca^{2+} homoestasis (Lew *et al.*, 2008).

In *Ca. albicans* Mid1 forms a complex with the voltage-gated Ca^{2+} channel Cch1 (Brand *et al.*, 2007); Mid1 is probably activated by membrane stretching and mediates the subsequent opening of the Cch1 channel, thus leading to localized Ca^{2+} influx. A reduced growth rate has been observed in *mid1*, *cch1* and the double knockout mutant, whereas the extension rate of hyphae remains unaffected. In addition, the ability of mutants to reorient growth when reaching a ridge is significantly reduced. On the other hand there are indications that, in *Saccharomyces cerevisiae*, the Mid1 channel itself is able to form a functional Ca^{2+} channel independent of Cch1 when heterologously expressed in hamster ovary cells (Kanzaki *et al.*, 1999).

Deletion of the *cch1* homologue in *Gibberella zeae* leads to reduced growth rate and a complete loss of ascospore discharge (Hallen & Trail, 2008). So far not much is known about the role of Mid1 homologues in plant-pathogenic fungi. A wide-scale silencing approach on several Ca^{2+}-signalling related proteins in *Magnaporthe grisea* (Nguyen *et al.*, 2008) revealed a minor role for both Mid1 and Cch1 in both pathogenicity and growth rate. Since this knock-down approach only diminishes the expression of both proteins compared to the wild-type, the results can only hint at the influence of these Ca^{2+} channels during plant infection.

Here we show that deletion of the *mid1* homologue in *Cl. purpurea* has a severe impact on pathogenicity, development and morphology.

METHODS

Strains and cultures. A derivative strain of *Claviceps purpurea* 20.1 (Hüsgen *et al.*, 1999), itself derived from the T5 strain isolated from *Secale cereale*, was used for generation of mutants and as reference strain for control experiments. In this strain (20.1Δ*ku70*), the *ku70* gene responsible for nonhomologous end joining (NHEJ) had been deleted (Haarmann *et al.*, 2008), drastically increasing the rate of homologous integration from 1–2 % to 50–60 %. For strain conservation, DNA isolation and spore production mycelia were grown on the complete medium BII (Esser & Tudzynski, 1978) or Mantle medium (MM; Mantle & Nisbet, 1976). For RNA isolation, submerged cultures of BII and MM were used. *Escherichia coli* strain TOP10 F′ was used for all cloning experiments. *E. coli* strain LE392 was used for reproduction of *Cl. purpurea* genomic lambda clones.

Nucleic acid extraction and analysis. Standard recombinant DNA methods were performed according to Ausubel *et al.* (1987) and Sambrook *et al.* (1989). Genomic DNA of *Cl. purpurea* was extracted from lyophilized mycelium as described by Cenis (1992). RNA for RT-PCR and Northern hybridization was isolated using the RNAgents total RNA isolation system from Promega. For RT-PCR 1 μg of total RNA was taken for cDNA synthesis using the oligo$(dT)_{12–18}$ primer and SuperScript II reverse transcriptase (Invitrogen) according to the manufacturer's instructions. PCR was performed in accordance with Sambrook *et al.* (1989), using Biotherm polymerase (Sigma). Primers were synthesized by Operon Biotechnologies. PCR fragments were cloned using the Invitrogen pCR2.1-TOPO-cloning kit. Southern and Northern blotting were performed on Amersham Hybond-N+ membrane according to the manufacturer's instructions. The membranes were hybridized with [α^{32}-P]dCTP-marked probes. Probes of genes were amplified by PCR. DNA sequencing was done (i) using the Thermo Sequenase fluorescent labelled primer cycle sequencing kit with 7deaza-dGTP (Amersham) and a LI-COR DNA sequencer models 4000 and 4200 (MWG Biotech) and (ii) using the Big Dye Terminator v3.1 sequencing kit (Applied Biosystems). For the latter method 200–250 ng plasmid DNA was applied. After the PCR the samples were purified by column chromatography and sequenced in an ABI Prism capillary sequencer (model 3730). Sequence alignments, editing and organization were done using either Lasergene software (DNAStar) or Vector NTI 10.3.0 (Invitrogen). Homology searches were performed with BLAST at NCBI (Altschul *et al.*, 1990).

Cloning of *mid1* and generation of replacement and complementation vector. A 918 bp fragment was obtained from a cDNA clone of a *Cl. purpurea* EST library (Oeser *et al.*, 2009) which showed a high similarity to *mid1* in *Neurospora crassa*, *Aspergillus fumigatus* and *Schizosaccharomyces pombe*. In order to obtain additional sequence information this fragment was used as a probe to screen a genomic library of *Cl. purpurea* strain T5 (Smit & Tudzynski, 1992) by plaque filter hybridization (Sambrook *et al.*, 1989). Of the 40 000 λ clones screened, 12 hybridized with the cDNA fragment. Three of these were further purified and subsequently analysed. After isolation from phages, DNA was digested with *Bam*HI, *Eco*RI, *Hin*dIII, *Sph*I, *Xba*I and *Xho*I. Fragments that showed positive hybridization with the *mid1* probe in the Southern analysis were cloned into pUC19 and subsequently sequenced. Two *Bam*HI fragments of about 1 kb and 2.5 kb and subclones from a 5 kb *Sph*I fragment gave rise to a total of 4862 bp of coding sequence and flanking region. Using this information, a replacement vector was constructed using primers 1 and 2 for amplification of 1341 bp of the designated left flank and primers 3 and 4 for amplification of 835 bp of the designated right flank of the replacement vector, respectively (Table 1 and Supplementary Fig. S1a). Both fragments were cloned into the pCR2.1-TOPO vector, sequenced using primers 15 and 16 (Table 1), excised using the restriction sites (*Hin*dIII/*Bgl*II and *Xba*I/*Sac*II, respectively) included in the 5′-ends of the primers (1 and 2 for the left flank and 3 and 4 for the right flank), and subsequently cloned upstream and downstream, respectively, of the phleomycin-resistance cassette of plasmid pAN81-UM (Müller *et al.*, 1997). Digestion of pΔmid1 with *Sac*II and *Hin*dIII released a 5521 bp fragment, which was used to transform the *Cl. purpurea* strain 20.1Δ*ku70*.

For complementation of Δ*mid1* mutant strains, the full-length coding region of *mid1* and an 850 bp segment upstream of the start codon were amplified from genomic DNA of *Cl. purpurea* strain 20.1Δ*ku70* using primers 11 and 12, respectively. The fragment was cloned into pCR2.1-TOPO vector, sequenced using primers 15 and 16 and subsequently excised using the *Apa*I/*Hin*dIII sites included in the 5′-ends of primers 11 and 12, respectively. The *Apa*I/*Hin*dIII fragment was cloned into vector pAN71-UM (Müller *et al.*, 1997), harbouring a hygromycin-resistance cassette, giving rise to the plasmid p7MeP. In order to achieve a recombination event *in loco*, a right flank

Downloaded from www.sgmjournals.org by
IP: 93.91.26.109
On: Wed, 02 Sep 2015 10:32:12

Table 1. PCR primers used in this study

No.	Sequence (5′→3′)
1	AGATCTCCGACGCCGTTTGACCA
2	TGGCTGTTCAAGCTTCCGTTCC
3	TCTAGATGAGACTCGGAAAGGCAGAAGATG
4	CCGCGGACACGTGGGCAG
5	ATGCGCCGAATATTGAGGATGACT
6	GCACCGGGGGAGGCTGAC
7	GCGTCTTCAAGTTCATTTTCCTC
8	GTTGTGACAGGACGAGGCTCCTCG
9	CCTATGAGTCGTTTACCCAGAATG
10	AGGCGACGCTCAGGAC
11	GGGCCCGAGGTGCCTGACTGGG
12	AAGCTTTCACCACACCACCAACAAGCC
13	TCTAGATGAGACTCGGAAAGGCAGAAGATG
14	CCGCGGACACGTGGGCAG
15	GAGCGGATAACAATTTCACACAGG
16	AGGGTTTTCCCAGTCACGACGGTT
17	GGGGCGTCGGTTTCCACTATCG

homologous to the right flank of the deletion vector was introduced. This flank was amplified using primers 13 and 14, digested using the artificial restriction sites included in the 5′-ends of the primers (*Xba*I, *Not*I), and ligated into vector p7MeP, yielding complementation vector p7cmid1.

Fungal transformation. Protoplast transformation was performed as described previously (Jungehülsing *et al.*, 1994). Protoplasts were generated using a mixture of lysing enzymes from *Trichoderma harzianum* and Driselase (both Sigma). For the gene replacement transformation, protoplasts were transformed with the fragment excised from pΔmid1 using *Sac*II and *Hin*dIII. Complementation was done by transformation with the fragment excised from p7cmid1 using *Apa*I and *Not*I. After transformation, protoplasts were mixed with 20 ml modified BII (pH 8, without $FeSO_4$, 20 %, w/v, sucrose) and poured into 92 mm Petri dishes. After 24 h incubation, a selective overlay of 10 ml BII medium containing either 100 μg phleomycin ml^{-1} (reaching a final concentration of 33 μg ml^{-1} on the transformation plates) for the *mid1* knockout or 1.5 mg hygromycin ml^{-1} (final concentration of 0.5 mg ml^{-1} on the transformation plate) for the complementation was applied. Resistant colonies were transferred to selection plates containing either 0.5 mg hygromycin ml^{-1} or 100 μg phleomycin ml^{-1}, depending on the resistance that was transferred. The gene replacement transformation was subsequently analysed by PCR for homologous integration of the fragment. To obtain homokaryotic knockout transformants, single-spore isolation was performed. Primer pairs used to identify transformants with homologous integration of the 5′ flank were 7 and 8, and for the 3′ flank 9 and 10 (Table 1 and Supplementary Fig. S1a). Complete deletion of *mid1* in the transformants was confirmed with the primer pair 5 and 6 (Table 1 and Supplementary Fig. S1a).

Plate assays. The base medium for all plate assays was MM. For each test at least five plates were prepared for each strain. Unless indicated elsewhere, the supplements were added prior to autoclaving. The pH was adjusted to 5.2 and a mycelial plug of either the reference strain 20.1Δ*ku70* or a mutant strain was placed in the middle of the plate.

For growth assays plates were prepared with agar of concentrations 1 %, 1.5 %, 2 % and 3 % (all w/v). To assess the role of elevated Ca^{2+} in the medium, MM was supplemented with 5, 10, 30, 40, 50, 100 and 200 mM $CaCl_2$. MM is usually supplemented with 4.2 mM $Ca(NO_3)_2$. For analysis of the effect of Ca^{2+} depletion, the medium was prepared without $CaCl_2$, and EGTA was added at concentrations of 1, 5 and 10 mM. Cell wall stress was tested with calcofluor white (CW) added in concentrations of 0.1, 0.25, 0.5, 0.75 and 1 mg ml^{-1} and Congo red (2 mg ml^{-1}), both after sterile filtration. The influence of osmotic stress was tested by adding NaCl at concentrations of 10, 50, 100, 500 mM and 1 M. Mg^{2+} was added as $MgSO_4$ at a concentration of 66 mM.

Measurements of the colony diameter were done after 14 days of growth under standard conditions, unless stated otherwise. Statistical analysis of group differences was done by use of the non-parametric Mann–Whitney *U*-test.

Pathogenicity tests. Rye plants were cultivated in growth chambers as described by Smit & Tudzynski (1992). Florets of blooming ears (30–40 per ear) were inoculated either with 5 μl of conidial suspension containing 2×10^6 viable spores ml^{-1} collected from MM agar, as described by Tenberge *et al.* (1996), or with a suspension of mycelium rubbed off an agar plate. Immediately after treatment the ears were covered with paper bags equipped with a cellophane window that allowed observation. *In vitro* pathogenicity tests were performed according to Scheffer & Tudzynski (2006). Isolated rye ovaries were cultivated on Hoagland medium (Hoagland & Arnon, 1950), modified for barley shoot culture (Scheffer & Tudzynski, 2006) and inoculated with a spore suspension (2×10^6 spores ml^{-1}) or mycelial suspension. At different time points the ovaries were dissected and stained with KOH/aniline blue (Currier & Strugger, 1956). This method allows detailed analysis of early infection stages (1–10 days post-inoculation; days p.i.) by epifluorescence microscopy (Hood & Shew, 1996). For scanning electron microscopy, ovaries were inoculated with each strain as described above. At 3 days p.i., samples were aldehyde fixed and dehydrated in an ethanol series as described by Giesbert *et al.* (1998). Samples were critical-point-dried (Emitech K850 critical point dryer), gold-sputtered (Emitech vacuum sputter device K550x) and examined with a Hitachi S.3000N scanning electron microscope at 15 kV.

Fig. 1. Amino acid sequence alignment of Mid1 orthologues of different filamentous fungi and yeasts: *Neurospora crassa* (CAD70927) (German Neurospora genome project, 2003), *Aspergillus fumigatus* (XP_754048) (Nierman *et al.*, 2005), *Neosartorya fischeri* (XP_001266052) (direct submission), *Aspergillus clavatus* (XP_001273916) (direct submission), *Aspergillus nidulans* (AAM47511) (direct submission), *Schizosaccharomyces pombe* (Q10063) (Tasaka *et al.*, 2000), *Sacccharomyces cerevisiae* (BAA06859) (Iida *et al.*, 1994) and *Claviceps purpurea*. Sequence alignment was done with CLUSTAL W of the DNAStar sequence analysis package using standard parameters. Grey shading indicates conserved amino acids; black shading indicates similar amino acids. The four potential transmembrane domains in *Cl. purpurea* are underlined. + indicates cysteine residues that are believed to be essential for function in *Sac. cerevisiae*, − those that are dispensable and ± those that are intermediate according to Maruoka *et al.* (2002). Diamonds (◇) indicate *N*-glycosylation sites of *Sac. cerevisiae* Mid1 (Iida *et al.*, 1994), of which some are conserved in *Cl. purpurea*. ↓ indicates conserved cysteine residues. The tryptophan residue marked with a horizontal arrow indicates the position from which in *Sac. cerevisiae* a truncation leads to loss of function (Maruoka *et al.*, 2002).

Downloaded from www.sgmjournals.org by
IP: 93.91.26.109
On: Wed, 02 Sep 2015 10:32:12

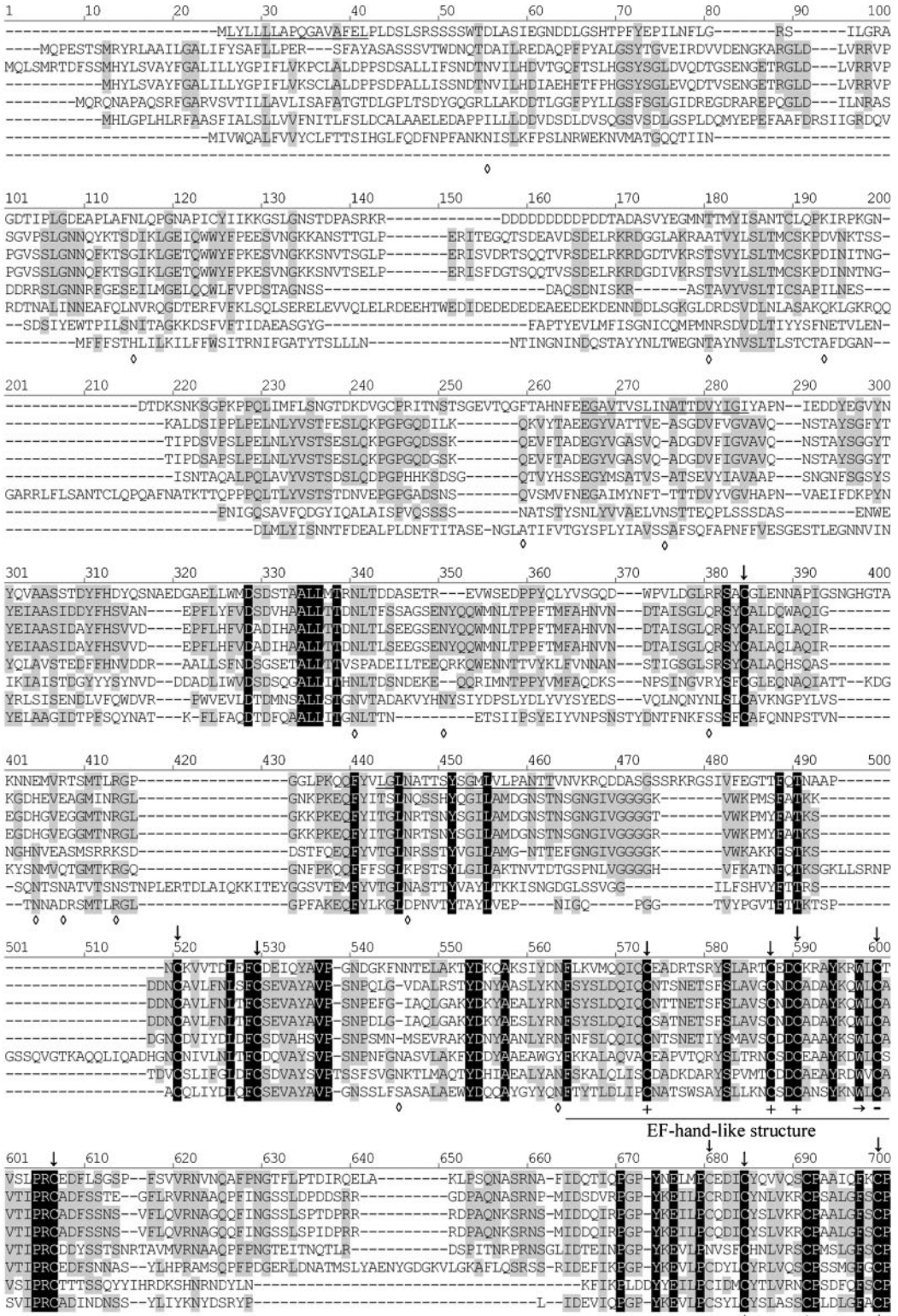

Downloaded from www.sgmjournals.org by
IP: 93.91.26.109
On: Wed, 02 Sep 2015 10:32:12

Microscopic analysis. The infected and KOH/aniline blue-stained ovaries were observed using epifluorescence microscopy (Leica DMRBE), equipped with a PixelFly Digital camera (PCO Computer Optics), using filter block A [excitation filter BP 340–380 (UV light), RKP 400, suppression filter LP 425]. For microscopic analysis of fungal hyphal structure, protoplasts or mycelial fragments of the respective strains were grown on agar-coated slides for 24 h in glass Petri dishes. CW staining of hyphae was done by incubating the whole slide for 10 min in CW (0.1 %, w/v, in 0.1 M Tris/HCl pH 8.5). Slides were washed twice with distilled water and observed with an inverted microscope (Leica DMIRE2) equipped with a Leica TCS SP2 laser-scanning device (Leica Microsystems) using a 40× (NA 0.8) water-immersion lens. CW fluorescence was excited using a 405 nm laser. Fluorescein isothiocyanate-labelled wheatgerm agglutinin (FITC-WGA) fluorescence was excited using a 498 nm laser line. Images were collected with 8-bit resolution using an emission range between 420 and 810 nm (CW) and 500 and 580 nm (FITC-WGA) with a frame average of 1 and a line average of 2. Electronic magnification was set at 4.7×. Images are shown as an average of five images.

RESULTS

Cl. purpurea mid1 encodes a putative stretch-activated, nonselective Ca^{2+} ion channel

A 918 bp fragment with high similarity to the *mid1* gene of *N. crassa* was obtained from a cDNA clone of an EST library of *Cl. purpurea* (Oeser *et al.*, 2009) and was used to screen a genomic λ library. Homologous fragments were subcloned and sequenced. The *mid1* gene in *Cl. purpurea* comprised two exons with a total length of 1899 bp and one intron of 117 bp (GenBank accession no. FM945328). The inferred 623 amino acid protein sequence contained all conserved domains typical for Mid1 (Fig. 1): four putative transmembrane domains, multiple *N*-glycosylation sites and ten conserved cysteine residues, of which four are reported to be essential, three are intermediate (meaning not necessarily important for function) and three are non-essential for function and localization in *Sac. cerevisiae* (Iida *et al.*, 1994; Maruoka *et al.*, 2002; Ozeki-Miyawaki *et al.*, 2005). Two of four hydrophobic transmembrane domains were located at the N- and the C-termini. The second hydrophobic domain (E^{200} to I^{218}) matched the third hydrophobic domain (H3) in *Sch. pombe* $Yam8^{+}$ and the third hydrophobic domain (L^{352} to L^{371}) matched the fourth hydrophobic domain (H4) in *Sac. cerevisiae* Mid1 with respect to position. Moreover, a cysteine-rich region at the C-terminus of the protein (C^{457} to C^{595}) is conserved and was shown to play an important role in protein–protein interactions in *Sac. cerevisiae* (Iida *et al.*, 1994). According to Maruoka *et al.* (2002) the *Sac. cerevisiae* homologue has an EF-hand-like structure spanning from F^{408} to V^{445} (corresponding to F^{448} to V^{485} in *Cl. purpurea*; Fig. 1) which includes three conserved cysteine residues (C^{417}, C^{431} and C^{434} in *Sac. cerevisiae*; C^{457}, C^{471} and C^{474} in *Cl. purpurea*) and which has a very low affinity for Ca^{2+} binding compared to the reference calmodulin. The region spanning from L^{487} to A^{508} (Fig. 1) showed similarity to the S3/H3 hydrophobic region of a superfamily of ion channels that consists of a cGMP-gated channel and several voltage-gated K^{+}, Na^{+} and Ca^{2+} channels (Jan & Jan, 1990). The amino acid sequence of the *Cl. purpurea* Mid1 showed 40.6 % identity to *Sac. cerevisiae* Mid1 (GenBank accession no. NP_014108), 48.8 % with *N. crassa* Mid1 (CAD70927) and 41.9 % to *Ca. albicans* Mid1 (XP_710952).

Generation of Δ*mid1* mutants

In order to study the impact of Mid1 on pathogenicity and development of *Cl. purpurea*, *mid1* was deleted by gene replacement (Supplementary Fig. S1a). For this purpose the 5′- and the 3′-flanking regions were amplified by PCR and subsequently fused to a phleomycin-resistance cassette. The excised replacement fragment was used to transform protoplasts of *Cl. purpurea* strain 20.1Δ*ku70*, a strain with an enhanced homologous recombination rate (Haarmann *et al.*, 2008). Phleomycin-resistant colonies were collected and analysed by diagnostic PCR. Five out of ten independent transformants showed homologous integration of the replacement fragment but – as usual for primary transformants of *Cl. purpurea* – amplification of the wild-type sequence indicated that these strains were heterokaryotic. A Southern blot experiment using three primary transformants showed a single integration at the designated gene locus as well as a weak wild-type signal (data not shown). Repeated single-spore isolations were performed to obtain homokaryotic deletion mutants, from which three stable homokaryotic deletion mutants were selected, Δ*mid1*-1, Δ*mid1*-2 and Δ*mid1*-3. Each mutant contained the 1.6 kb PCR fragment specific to the left flank and the 1.3 kb right flank fragment, but lacked the 0.9 kb wild-type fragment (*mid1*; Supplementary Fig. S1b). No wild-type signal was observed in Southern analysis (Supplementary Fig. S1c). Since all transformants showed a similar phenotype in terms of pathogenicity, growth rate and morphology (data not shown), the mutant Δ*mid1*-2 was selected for further investigation and for complementation (hereinafter referred to as the Δ*mid1* mutant strain).

Deletion of *mid1* leads to a significant growth defect in axenic culture

The Δ*mid1* mutant showed normal colony morphology compared to 20.1Δ*ku70* on different growth media, but a significantly lower growth rate (Fig. 2a). After 12 days of growth on MM the mean colony diameter was 63 ± 0.77 mm for 20.1Δ*ku70* and 44 ± 2 mm for Δ*mid1*.

In contrast to *Sac. cerevisiae* (Iida *et al.*, 1994), it was not possible to complement this phenotype by supplementation of the growth medium with higher concentrations of $CaCl_2$ (up to 200 mM). In fact the growth rate compared to 20.1Δ*ku70* was further reduced by higher Ca^{2+} concentrations (Supplementary Fig. S2). Similarly, supplementing the medium with Mg^{2+} (66 mM) decreased the mean growth rate to about 45 % that of 20.1Δ*ku70* (28.4 ± 1.72 mm; data not shown).

Downloaded from www.sgmjournals.org by
IP: 93.91.26.109
On: Wed, 02 Sep 2015 10:32:12

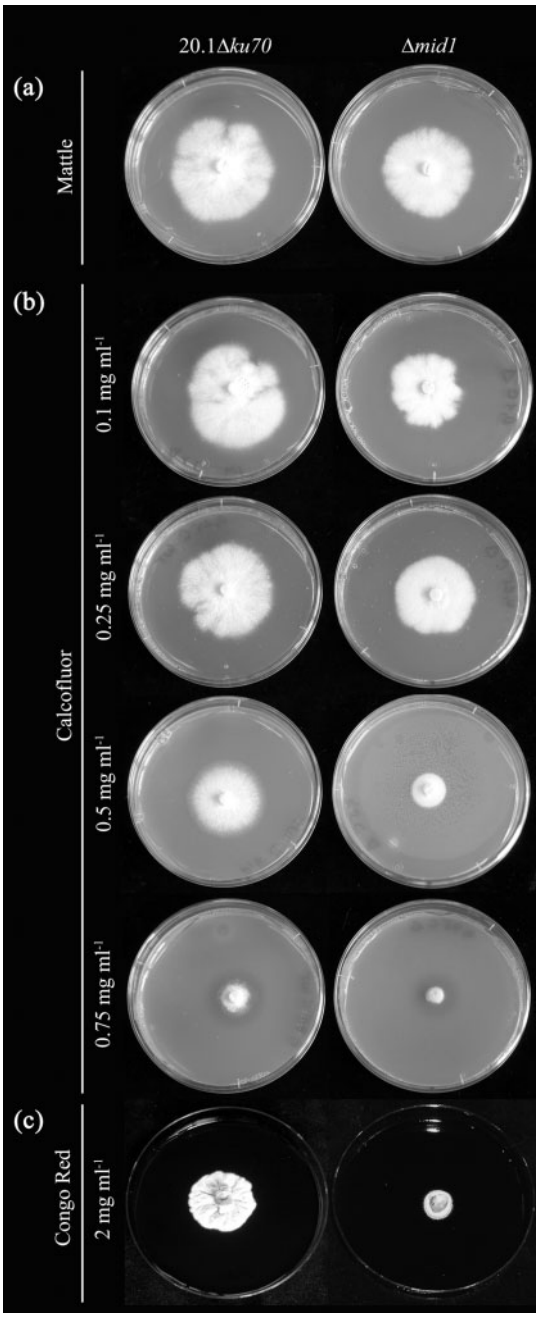

Fig. 2. Colony morphology of 20.1Δ*ku70* and the Δ*mid1* mutant on MM (a), MM with CW (b) and MM with Congo red (c) after 1 week of growth. In all conditions tested the growth of the Δ*mid1* mutant is reduced compared to that of 20.1Δ*ku70*.

The growth defect of Δ*mid1* could be partially complemented with increased agar concentration in MM (1 %, 1.5 %, 2 %, 3 % agar; all w/v, Supplementary Fig. S3). Whereas 20.1Δ*ku70* showed a consistent growth pattern over the four agar densities tested (44 ± 1.52 mm, 9 days p.i.), the Δ*mid1* mutant showed a significantly increased growth rate from 26 ± 1.41 mm at 1 % agar to 33 ± 2 mm at 3 % agar (Supplementary Fig. S3b). However, increased agar concentration did not lead to the full restoration of 20.1Δ*ku70* growth.

The Δ*mid1* mutant shows higher sensitivity to cell wall stress but not to osmotic stress

Since Mid1 in other systems is known to be involved in sensitivity to cell wall and osmotic stress, plate assays with standard stressors were performed. Both Congo red (2 mg ml^{-1}; Fig. 2c) and CW (0.1–0.75 mg ml^{-1}; Fig. 2b), which interfere with cell wall structure, had a significant effect on the growth rate of the Δ*mid1* mutant.

Because of these effects, cell wall morphology was investigated by fluorescence microscopy using CW, a fluorochrome that interacts with several (mostly β-1,4-linked) polysaccharides (Maeda & Ishida, 1967; Pringle, 1991) and can be used to stain the fungal cell wall. Massive aggregations of cell wall polysaccharides were observed randomly distributed over the hyphae of the Δ*mid1* mutant after 10 min incubation in CW solution. In most cases, the septa appeared thicker in the Δ*mid1* mutant (Fig. 3a). Furthermore, a diffuse accumulation of cell wall material was observed in hyphal tips (Fig. 3c, d). This accumulation was less pronounced in the very tip of growing hyphae of the Δ*mid1* mutant compared to hyphae of 20.1Δ*ku70*. In the Δ*mid1* mutant the CW fluorescence predominantly accumulated in a ring adjacent to the apex (Fig. 3c). Fluorescence microscopy with FITC-WGA, which has a high affinity for β-linked polymers of *N*-acetylglucosamines like chitin (Meyberg, 1988; Schoffelmeer *et al.*, 1999), suggests that these aggregates do not contain chitin (Fig. 3g, h).

Both 20.1Δ*ku70* and the Δ*mid1* mutant showed a decrease in growth rate under NaCl-induced osmotic stress. However, at concentrations up to 100 mM, the growth of Δ*mid1* was actually less impaired than that of20.1Δ*ku70*. Growth rates of both the mutant and 20.1Δ*ku70* were impaired at 0.5 M NaCl, and growth ceased at concentrations in excess of 1 M NaCl (Supplementary Fig. S4).

Mid1 affects Ca^{2+} homeostasis

A plate assay using MM (without $CaCl_2$ supplementation) and different concentrations of the Ca^{2+} chelator EGTA (0, 1, 5 and 10 mM) revealed that the Δ*mid1* mutant has a higher tolerance of reduced external Ca^{2+} concentrations than did 20.1Δ*ku70*. At lower concentrations of EGTA and on plates without $CaCl_2$, 20.1Δ*ku70* showed a greater reduction in growth rate than the mutant, while significant growth inhibition in the mutant was only observed at the highest EGTA concentration of 10 mM (Supplementary Fig. S5). Growth of the Δ*mid1* mutant was also inhibited by elevated intracellular Ca^{2+} concentrations, as shown by growth assays using the ionophore A23187, which increases intracellular Ca^{2+} levels (Nelson *et al.*, 2004). Filter papers soaked with 9.5 mM ionophore in ethanol were applied to

Downloaded from www.sgmjournals.org by
IP: 93.91.26.109
On: Wed, 02 Sep 2015 10:32:12

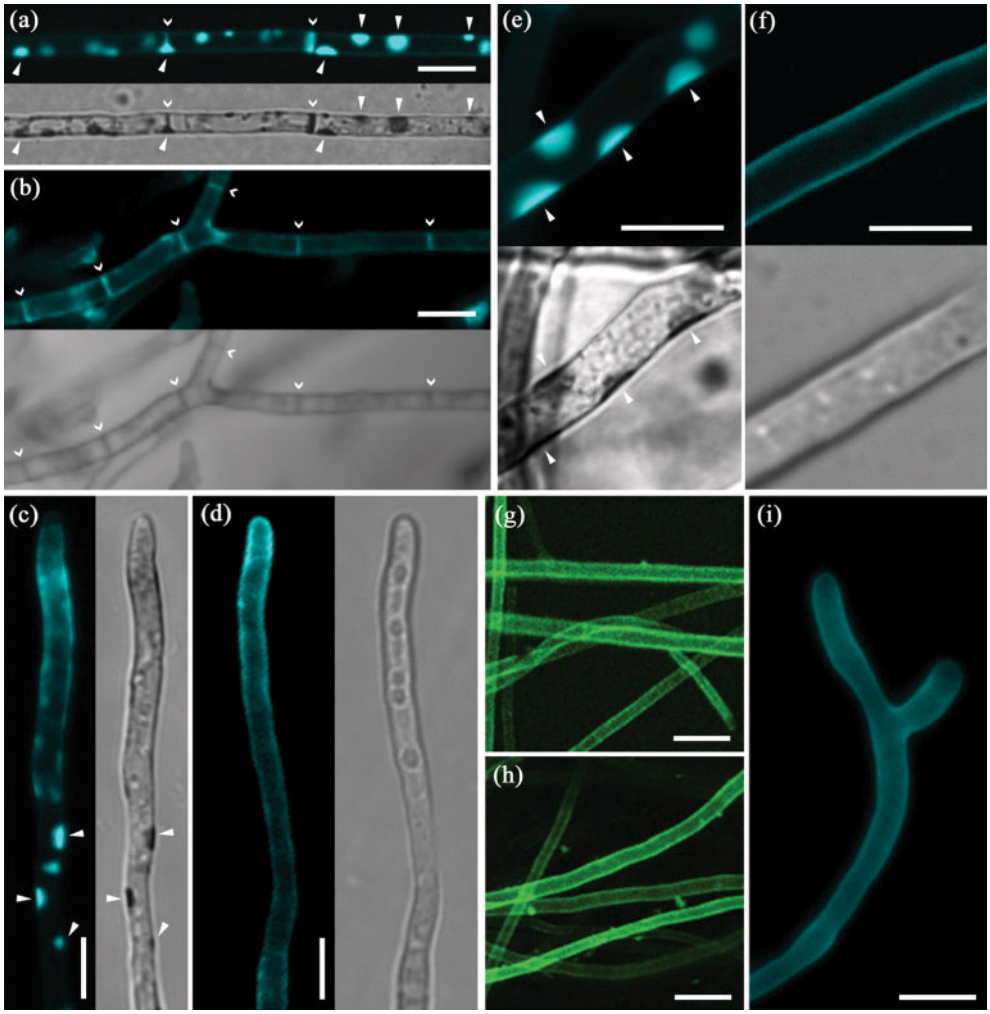

Fig. 3. Confocal laser scanning microscopy: CW and FITC-WGA staining of hyphae of the Δ*mid1* mutant and 20.1Δ*ku70* in the fluorescence channel and differential interference contrast (DIC). (a, b) CW fluorescence reveals regular septation (open arrowheads) in both the Δ*mid1* mutant (a) and 20.1Δ*ku70* (b). (a) In the DIC micrograph opaque aggregations (arrowheads) and a thickened septum (open arrow in the middle of the micrograph) can be seen in hyphae of the Δ*mid1* mutant. CW fluorescence indicates a high content of cell wall polysaccharides in these aggregations. (b) DIC and CW fluorescence show no abnormalities in the distribution of cell wall polysaccharides in 20.1Δ*ku70.* Higher magnifications of CW-stained Δ*mid1* mutant and 20.1Δ*ku70* hyphae are shown in (e) and (f), respectively. (c) A ring of fluorescence accumulation can be seen adjacent to the growing apex of a Δ*mid1* mutant hypha. (d) Fluorescence accumulates at the very tip of a growing hypha of 20.1Δ*ku70.* (g, h) FITC-WGA staining shows similar uniform distribution of chitin in hyphae of the Δ*mid1* mutant (g) and 20.1Δ*ku70* (h). (i) CW staining of a hypha of the complemented Δ*mid1* mutant. Scale bars, 10 μm.

MM agar plates supplemented with 4.2, 10, 30, 40, 50 and 100 mM $CaCl_2$ and inoculated with 20.1Δ*ku70* and Δ*mid1*. After 2 weeks, both 20.1Δ*ku70* and the mutant strain were able to grow towards and across the control filter papers (ethanol only). A zone of inhibition was observed around the ionophore filter papers on plates inoculated with the Δ*mid1* mutant, whereas 20.1Δ*ku70* was able to grow around the paper with little or no inhibition (Fig. 4). The increase in Ca^{2+} concentration in the medium had no additional impact on the effect of A23187 (data not shown). Both results indicate a role for *Cl. purpurea* Mid1 in environmental Ca^{2+} sensing.

The Δ*mid1* mutant is unable to infect rye

Two types of pathogenicity assays were performed to test the virulence of Δ*mid1* mutant: blooming rye ears or isolated rye ovaries were inoculated with either a suspension of mycelial fragments or with spores of 20.1Δ*ku70* and the Δ*mid1* mutant (Scheffer & Tudzynski,

Downloaded from www.sgmjournals.org by
IP: 93.91.26.109
On: Wed, 02 Sep 2015 10:32:12

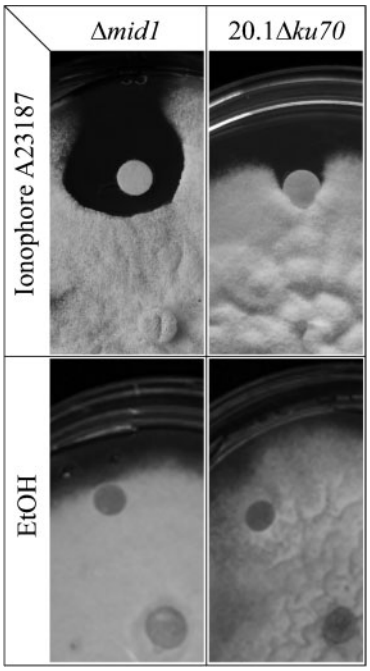

Fig. 4. Effect of the ionophore A23187 on the growth of 20.1Δ*ku70* and the Δ*mid1* mutant. Colonies were grown for 2 weeks on MM. Filter papers soaked with either ethanol (EtOH) or the ionophore were placed along the growing edge of the colony.

2006). Since the Δ*mid1* mutant spores show a slightly reduced germination rate, the conidial titre was adjusted in order to ensure that the same amount of viable spores was applied to the plant. In the *in planta* tests, rye florets infected with 20.1Δ*ku70* spores or mycelial fragments showed a typical infection time-course and development of infection structures (honeydew after 8 ± 1 days p.i., sclerotia formation after 16–23 days p.i.). In contrast, rye florets infected with either spores or hyphal fragments of the Δ*mid1* mutant showed no symptoms of infection. The *in vitro* infection test confirmed these results. A time-course experiment showed no sign of infection on isolated ovaries up to 10 days p.i., either in the style or in the transmitting tissue (Fig. 5). Scanning electron microscopy revealed that the Δ*mid1* mutant builds an appressorium-like structure that is unusual for *Cl. purpurea* (Fig. 6d). From this structure the fungus grows in many directions, showing hyperbranching across the surface of the rye stigma (Figs 6d, e and 5h, j).

These findings strongly suggest that Mid1 is required for invasion of the host tissue and thus represents a pathogenicity factor. To confirm that this phenotype is indeed due to the deletion of *mid1*, the mutant was complemented using the vector p7cmid1. In the complemented Δ*mid1* mutant, *mid1* expression was verified by Northern hybridization (data not shown) and RT-PCR (Supplementary Fig. S1d). The complemented Δ*mid1* mutant showed normal growth and was able to infect rye ovaries (Fig. 5k). The defect in cell wall composition was also abolished (Fig. 3i).

DISCUSSION

We have shown that the putative Ca^{2+} channel Mid1 is essential for penetration of the host tissue by *Cl. purpurea*. The penetration defect shown by the Δ*mid1* mutant could be due to disturbed sensing or reduced ability to generate the necessary mechanical force. The thigmotrophic response of *Ca. albicans* to varying surface contours can be attenuated when gadolinium (Gd^{3+}), a blocker of stretch-activated ion channels (Kanzaki *et al.*, 1999; Watts *et al.*, 1998) is applied or the genes proposed to be responsible (*Camid1* and *Cacch1*) are deleted (Watts *et al.*, 1998; Brand *et al.*, 2007). Surprisingly, Gd^{3+} seems to have no impact on vegetative growth in *Cl. purpurea* (data not shown); this is in accordance with the findings in *N. crassa* (Levina *et al.*, 1995). Hence it is likely that membrane-localized stretch-activated Ca^{2+} channels, and therefore Ca^{2+} influx, are not essential for tip growth. It is conceivable that mechanical force plays a major role in thigmotropism since the membrane is stretched during invasive growth (Read *et al.*, 1992), whether into agar, a plant cell (e.g *Cl. purpurea*) or human tissue (e.g *Ca. albicans*). The slight increase in growth performance of the Δ*mid1* mutant on plates with a higher agar concentration also indicates an involvement of Mid1 in thigmotropism since the fungus is growing on the surface of the agar rather than invading the agar as it would at the lower agar concentration of 1.5 %. The deletion of the gene encoding the NDR-like kinase Cot1 in *Cl. purpurea* led to a growth phenotype comparable to that of Δ*mid1* (Scheffer *et al.*, 2005). This phenotype could be partially suppressed by the use of a high agar concentration in an overlay, indicating that pressure and mechanical stress also play a role in vegetative growth in *Cl. purpurea*. In contrast, data from Lew *et al.* (2008) in *N. crassa* suggest the opposite conclusion, that harder agar has no impact on growth rate in the Δ*Ncmid1* mutant. However, in addition to the use of a different experimental design, it is also feasible that there is a fundamental difference in Mid1 function between saprophytic and plant-pathogenic fungi. Conflicting results were also obtained for the effects of Ca^{2+} depletion in the medium: whereas Ca^{2+} depletion leads to growth arrest in the *N. crassa mid1* mutant (Lew *et al.*, 2008), the *Cl. purpurea mid1* mutant was less sensitive to Ca^{2+} depletion than 20.1Δ*ku70*. In this case it is possible that intracellular Ca^{2+} stores partially complement the Ca^{2+} depletion. This assumption is supported by the finding that a reduction of extracellular Ca^{2+} concentrations by EGTA has almost no effect on the growth rate of the Δ*mid1* mutant up to an EGTA concentration of 5 mM. These results suggest that Mid1 plays a role in sensing of both surface characteristics and environmental Ca^{2+} concentrations.

Downloaded from www.sgmjournals.org by
IP: 93.91.26.109
On: Wed, 02 Sep 2015 10:32:12

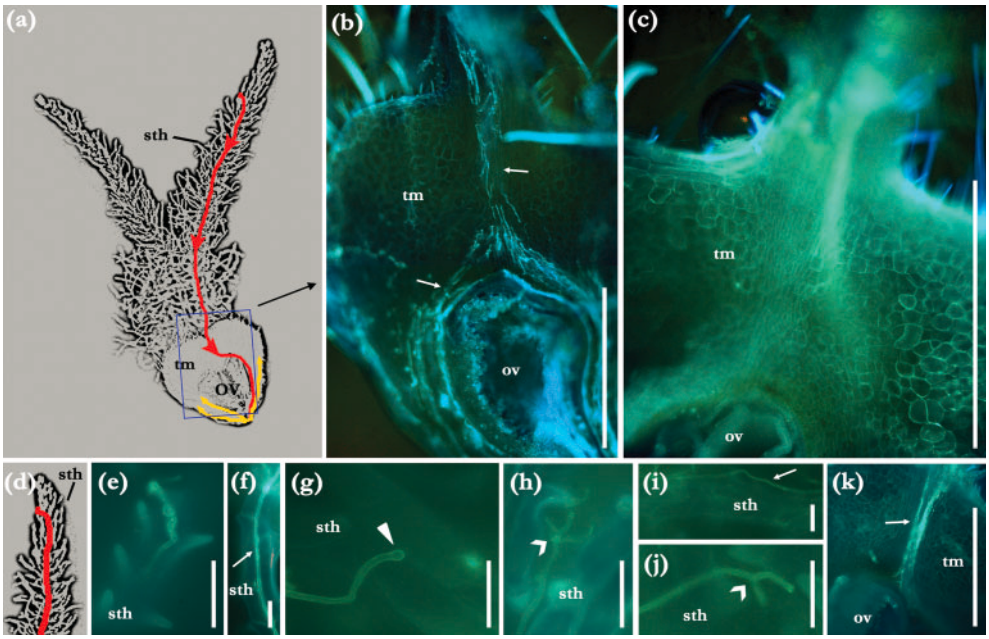

Fig. 5. *In vitro* pathogenicity test: KOH/aniline blue staining. (a) Scheme of fungal growth within the rye ovary (6–7 days p.i.). Early infection is shown by red arrows; yellow arrows indicate spreading hyphae starting to colonize the whole ovary after tapping into the vascular bundles of the host plant. The blue box indicates the section shown in (b). (b) Micrograph of an ovary infected with 20.1Δ*ku70* (4 days p.i., assembled picture). The arrows indicate hyphae. (c) Micrograph of an ovary inoculated with the Δ*mid1* mutant (4 days p.i.). (d) Scheme of fungal growth within the rye style. Early infection path is indicated by the red line. (e–j) Stigmatic hairs in higher magnification infected with either 20.1Δ*ku70* (e, f) or the Δ*mid1* mutant (g–j) of *Cl. purpurea*. (e) Germinated spore of 20.1Δ*ku70* invading the stigmatic hair. (f) Hypha of 20.1Δ*ku70* growing inside a stigmatic hair (arrow). (g) Hypha of the Δ*mid1* mutant forming an appressorium-like structure (arrowhead). No subsequent invasion of the stigma can be seen. (h) Multiple outgrowths out of an appressorium-like structure (open arrowhead). (i) Hypha of the Δ*mid1* mutant growing over the surface of the stigmatic hair (solid arrowhead). (j) Branching of a hypha growing over a stigmatic hair (open arrowhead). (k) Micrograph of an ovary infected with the complemented Δ*mid1* mutant (5 days p.i., assembled picture). The arrows indicate hyphae. Scale bars: in (b) and (c), 1 mm; in (e–k), 20 μm. sth, stigmatic hair; tm, transmitting tissue; ov, ovule.

The reduced growth rate *in vitro* might be due to alterations in the cell wall. The cell wall of yeasts and filamentous fungi consists of a fibrillar network of polysaccharides (the most prominent of which are β-1,3-glucans) that protects the cell from external stress and also maintains cell shape and flexibility (de Nobel *et al.*, 2001). The reduced accumulation of cell wall polysaccharides in growing tips of the Δ*mid1* mutant may be one explanation for the reduced growth rate. Hyphal elongation depends on accurate transport and deposition of cell wall material towards the growing apex (reviewed by Fischer *et al.*, 2008; Harris & Momany, 2004). This process seems to be disturbed when *mid1* is deleted. Carnero *et al.* (2000) showed that a mutation in the *Sch. pombe* homologue of Mid1 (ehs1p) causes an imbalance in the polysaccharide content of the cell wall. The authors observed a more intense CW fluorescence at distinct foci and thickened septa due to an increase in β-glucan content in the cell wall. Our microscopic observations strongly suggest a comparable modification in the cell wall content of the Δ*mid1* mutant in *Cl. purpurea*.

A region of the *Cl. purpurea* Mid1 amino acid sequence (F^{448} to V^{485}) shows low similiarity to an EF-hand domain in the *Sac. cerevisiae* Mid1 protein. In *Sac. cerevisiae* the comparable region has a low affinity for Ca^{2+}, is needed for Mid1 function, and is believed to play a role in protein–protein interactions (Maruoka *et al.*, 2002). Mid1 may interact *in vivo* with the voltage-gated Ca^{2+} channel Cch1: it was shown previously that Mid1 either interacts with Cch1 or at least shares functional properties with it, as indicated by knockout of either gene in *Ca. albicans* (Brand *et al.*, 2007) and *Sac. cerevisiae* (Fischer *et al.*, 1997; Iida *et al.*, 2004; Paidhungat & Garrett, 1997).

The *Cl. purpurea* Δ*mid1* mutant shows a hyperbranching phenotype when growing on the surface of rye florets. It was shown previously that mutation of genes related to calcium signalling often causes hyperbranching of hyphae and hyphal tips (da Silva Ferreira *et al.*, 2007; Prokisch *et al.*, 1997). The same phenotype was observed in *Fusarium graminearum* when calcium signalling was chemically disrupted (Robson *et al.*, 1991). It seems likely

Downloaded from www.sgmjournals.org by
IP: 93.91.26.109
On: Wed, 02 Sep 2015 10:32:12

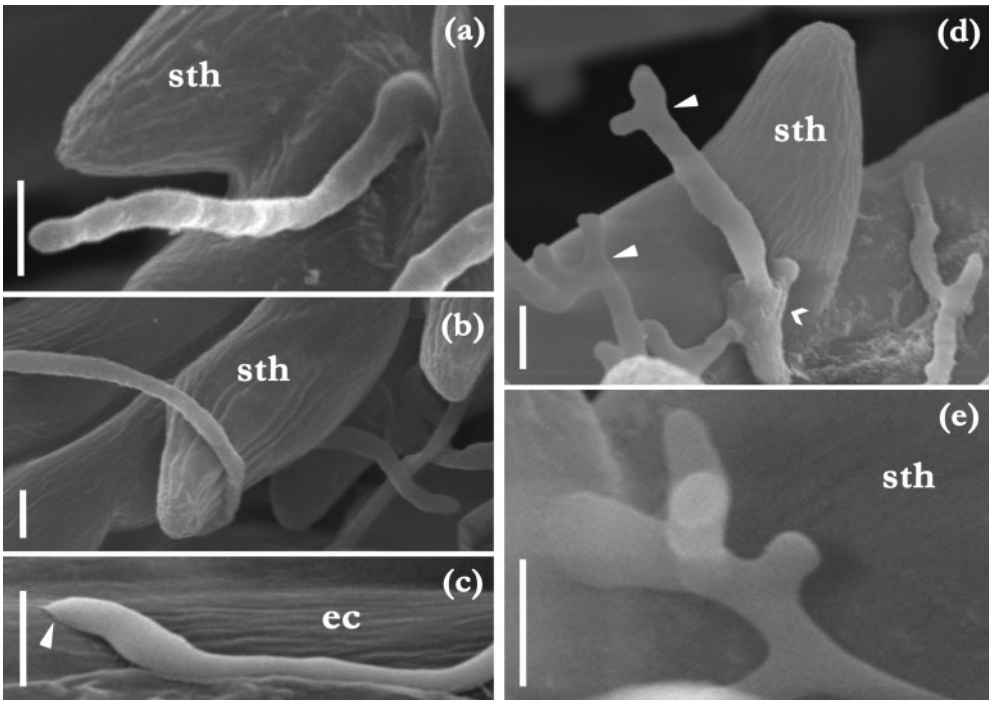

Fig. 6. Scanning electron microscopy of *in vitro* pathogenicity test. High-resolution images of rye ovaries after infection with 20.1Δ*ku70* (a–c) or the Δ*mid1* mutant (d–e). (a) Germinated 20.1Δ*ku70* spore growing on the surface of a stigmatic hair. (b) A 20.1Δ*ku70* hypha growing around a stigmatic hair. (c) A 20.1Δ*ku70* hypha penetrating an epidermal cell of the style (arrowhead). (d) Δ*mid1* mutant growing on the surface of the style and around a stigmatic hair, showing a hyperbranching phenotype. The open arrowhead indicates a swelling of the hyphae at the putative point of attempted penetration (appressorium-like structure) and multiple outgrowths from this structure. The solid arrowhead indicates a hypha with multiple branches. (e) A hypha of the Δ*mid1* mutant showing a hyperbranching phenotype when growing on the surface of a stigmatic hair. Scale bar, 10 μm. sth, stigmatic hair; ec, epidermal cells.

that in *Cl. purpurea* a Ca^{2+} signal is needed to penetrate the plant tissue, and Mid1 is a strong candidate for a role in perception of the signal on the plant surface.

ACKNOWLEDGEMENTS

We thank Sarah Brown for critical reading of the manuscript, M. Becker for assistance with scanning electron microscopy and the Deutsche Forschungsgemeinschaft (DFG; SFB 629 'Molecular cell dynamics') for financial support.

REFERENCES

Altschul, S. F., Gish, W., Miller, W., Myers, E. W. & Lipman, D. J. (1990). Basic local alignment search tool. *J Mol Biol* **215**, 403–410.

Ausubel, F. M., Brent, R., Kingston, R. E., Moore, D. D., Seidman, J. G., Smith, J. A. & Struhl, K. (1987). *Current Protocols in Molecular Biology.* New York: Wiley.

Brand, A., Shanks, S., Duncan, V. M., Yang, M., Mackenzie, K. & Gow, N. A. R. (2007). Hyphal orientation of *Candida albicans* is regulated by a calcium-dependent mechanism. *Curr Biol* **17**, 347–352.

Carnero, E., Ribas, J. C., García, B., Durán, A. & Sánchez, Y. (2000). *Schizosaccharomyces pombe* ehs1p is involved in maintaining cell wall integrity and in calcium uptake. *Mol Gen Genet* **264**, 173–183.

Cenis, J. L. (1992). Rapid extraction of fungal DNA for PCR amplification. *Nucleic Acids Res* **20**, 2380.

Currier, H. B. & Strugger, S. (1956). Aniline blue and fluorescence microscopy of callose in bulb scales of *Allium cepa* L. *Protoplasma* **45**, 552–559.

Cyert, M. S. (2003). Calcineurin signaling in *Saccharomyces cerevisiae*: how yeast go crazy in response to stress. *Biochem Biophys Res Commun* **311**, 1143–1150.

da Silva Ferreira, M. E., Heinekamp, T., Härtl, A., Brakhage, A. A., Semighini, C. P., Harris, S. D., Savoldi, M., de Gouvêa, P. F., de Souza Goldman, M. H. & other authors (2007). Functional characterization of the *Aspergillus fumigatus* calcineurin. *Fungal Genet Biol* **44**, 219–230.

de Nobel, H., Sietsma, J. H., van den Ende, H. & Klis, F. M. (2001). Molecular organization and construction of the fungal cell wall. In *The Mycota VIII: Biology of the Fungal Cell*, pp. 181–200. Edited by R. J. Howard & N. A. R. Gow. Berlin & Heidelberg: Springer.

Esser, K. & Tudzynski, P. (1978). Genetics of the ergot fungus *Claviceps purpurea. Theor Appl Genet* **53**, 145–149.

Fischer, M., Schnell, N., Chattaway, J., Davies, P., Dixon, G. & Sanders, D. (1997). The *Saccharomyces cerevisiae CCH1* gene is involved in calcium influx and mating. *FEBS Lett* **419**, 259–262.

Fischer, R., Zekert, N. & Takeshita, N. (2008). Polarized growth in fungi – interplay between the cytoskeleton, positional markers and membrane domains. *Mol Microbiol* **68**, 813–826.

Downloaded from www.sgmjournals.org by
IP: 93.91.26.109
On: Wed, 02 Sep 2015 10:32:12

Garrill, A., Jackson, S. L., Lew, R. R. & Heath, I. B. (1993). Ion channel activity and tip growth: tip-localized stretch-activated channels generate an essential Ca^{2+} gradient in the oomycete *Saprolegnia ferax*. *Eur J Cell Biol* **60**, 358–365.

Giesbert, S., Lepping, H. B., Tenberge, K. B. & Tudzynski, P. (1998). The xylanolytic system of *Claviceps purpurea*: cytological evidence for secretion of xylanases in infected rye tissue and molecular characterization of two xylanase genes. *Phytopathology* **88**, 1020–1030.

Haarmann, T., Lorenz, N. & Tudzynski, P. (2008). Use of a nonhomologous end joining deficient strain (Δ*ku70*) of the ergot fungus *Claviceps purpurea* for identification of a nonribosomal peptide synthetase gene involved in ergotamine biosynthesis. *Fungal Genet Biol* **45**, 35–44.

Hallen, H. E. & Trail, F. (2008). The L-type calcium ion channel cch1 affects ascospore discharge and mycelial growth in the filamentous fungus *Gibberella zeae* (anamorph *Fusarium graminearum*). *Eukaryot Cell* **7**, 415–424.

Harris, S. D. & Momany, M. (2004). Polarity in filamentous fungi: moving beyond the yeast paradigm. *Fungal Genet Biol* **41**, 391–400.

Hepler, P. K., Vidali, L. & Cheung, A. Y. (2001). Polarized cell growth in higher plants. *Annu Rev Cell Dev Biol* **17**, 159–187.

Hoagland, D. R. & Arnon, D. I. (1950). The water-culture method for growing plants without soil. In *Agricultural Experimental Station Circular 347*. Berkley, CA: College of Agriculture, University of California.

Hood, M. E. & Shew, H. D. (1996). Applications of KOH-aniline blue fluorescence in the study of plant-fungal interactions. *Phytopathology* **86**, 704–708.

Hüsgen, U., Büttner, P., Müller, U. & Tudzynski, P. (1999). Variation in karyotype and ploidy level among field isolates of *Claviceps purpurea*. *J Phytopathol* **147**, 591–597.

Iida, H., Nakamura, H., Ono, T., Okumura, M. S. & Anraku, Y. (1994). *MID1*, a novel *Saccharomyces cerevisiae* gene encoding a plasma membrane protein, is required for Ca^{2+} influx and mating. *Mol Cell Biol* **14**, 8259–8271.

Iida, K., Tada, T. & Iida, H. (2004). Molecular cloning in yeast by in vivo homologous recombination of the yeast putative α1 subunit of the voltage-gated calcium channel. *FEBS Lett* **576**, 291–296.

Jackson, S. L. & Heath, I. B. (1993). Roles of calcium ions in hyphal tip growth. *Microbiol Rev* **57**, 367–382.

Jan, L. Y. & Jan, Y. N. (1990). A superfamily of ion channels. *Nature* **345**, 672.

Jungehülsing, U., Arntz, C., Smit, R. & Tudzynski, P. (1994). The *Claviceps purpurea* glyceraldehyde-3-phosphate dehydrogenase gene: cloning, characterization, and use for the improvement of a dominant selection system. *Curr Genet* **25**, 101–106.

Kanzaki, M., Nagasawa, M., Kojima, I., Sato, C., Naruse, K., Sokabe, M. & Iida, H. (1999). Molecular identification of a eukaryotic, stretch-activated nonselective cation channel. *Science* **285**, 882–886.

Kraus, P. R. & Heitman, J. (2003). Coping with stress: calmodulin and calcineurin in model and pathogenic fungi. *Biochem Biophys Res Commun* **311**, 1151–1157.

Levina, N. N., Lew, R. R., Hyde, G. J. & Heath, I. B. (1995). The roles of Ca^{2+} and plasma membrane ion channels in hyphal tip growth of *Neurospora crassa*. *J Cell Sci* **108**, 3405–3417.

Lew, R. R., Abbas, Z., Anderca, M. I. & Free, S. J. (2008). Phenotype of a mechanosensitive channel mutant, *mid*-1, in a filamentous fungus, *Neurospora crassa*. *Eukaryot Cell* **7**, 647–655.

Maeda, H. & Ishida, N. (1967). Specificity of binding of hexopyranosyl polysaccharides with fluorescent brightener. *J Biochem* **62**, 276–278.

Malhó, R. & Trewavas, A. J. (1996). Localized apical increases of cytosolic free calcium control pollen tube orientation. *Plant Cell* **8**, 1935–1949.

Mantle, P. G. & Nisbet, L. J. (1976). Differentiation of *Claviceps purpurea* in axenic culture. *J Gen Microbiol* **93**, 321–334.

Maruoka, T., Nagasoe, Y., Inoue, S., Mori, Y., Goto, J., Ikeda, M. & Iida, H. (2002). Essential hydrophilic carboxyl-terminal regions including cysteine residues of the yeast stretch-activated calcium-permeable channel Mid1. *J Biol Chem* **277**, 11645–11652.

Mattson, M. P. (1999). Establishment and plasticity of neuronal polarity. *J Neurosci Res* **57**, 577–589.

Meyberg, M. (1988). Selective staining of fungal hyphae in parasitic and symbiotic plant-fungus associations. *Histochemistry* **88**, 197–199.

Müller, U., Tenberge, K. B., Oeser, B. & Tudzynski, P. (1997). *Cel1*, probably encoding a cellobiohydrolase lacking the substrate binding domain, is expressed in the initial infection phase of *Claviceps purpurea* on *Secale cereale*. *Mol Plant Microbe Interact* **10**, 268–279.

Nakagawa, Y., Katagiri, T., Shinozaki, K., Qi, Z., Tatsumi, H., Furuichi, T., Kishigami, A., Sokabe, M., Kojima, I. & other authors (2007). *Arabidopsis* plasma membrane protein crucial for Ca^{2+} influx and touch sensing in roots. *Proc Natl Acad Sci U S A* **104**, 3639–3644.

Nelson, G., Kozlova-Zwinderman, O., Collis, A. J., Knight, M. R., Fincham, J. R., Stanger, C. P., Renwick, A., Hessing, J. G., Punt, P. J. & other authors (2004). Calcium measurement in living filamentous fungi expressing codon-optimized aequorin. *Mol Microbiol* **52**, 1437–1450.

Nguyen, Q. B., Kadotani, N., Kasahara, S., Tosa, Y., Mayama, S. & Nakayashiki, H. (2008). Systematic functional analysis of calcium-signalling proteins in the genome of the rice-blast fungus, *Magnaporthe oryzae*, using a high-throughput RNA-silencing system. *Mol Microbiol* **68**, 1348–1365.

Nierman, W. C., Pain, A., Anderson, M. J., Wortman, J. R., Kim, H. S., Arroyo, J., Berriman, M., Abe, K., Archer, D. B. & other authors (2005). Genomic sequence of the pathogenic and allergenic filamentous fungus *Aspergillus fumigatus*. *Nature* **438**, 1151–1156.

Oeser, B., Heidrich, P. M., Muller, U., Tudzynski, P. & Tenberge, K. B. (2002). Polygalacturonase is a pathogenicity factor in the *Claviceps purpurea*/rye interaction. *Fungal Genet Biol* **36**, 176–186.

Oeser, B., Beaussart, F., Haarmann, T., Lorenz, N., Nathues, E., Rolke, Y., Scheffer, J., Weiner, J. & Tudzynski, P. (2009). Expressed sequence tags from the flower pathogen *Claviceps purpurea*. *Mol Plant Pathol* **10**, 665–684.

Ozeki-Miyawaki, C., Moriya, Y., Tatsumi, H., Iida, H. & Sokabe, M. (2005). Identification of functional domains of Mid1, a stretch-activated channel component, necessary for localization to the plasma membrane and Ca^{2+} permeation. *Exp Cell Res* **311**, 84–95.

Paidhungat, M. & Garrett, S. (1997). A homolog of mammalian, voltage-gated calcium channels mediates yeast pheromone-stimulated Ca^{2+} uptake and exacerbates the cdc1(Ts) growth defect. *Mol Cell Biol* **17**, 6339–6347.

Pierson, E. S., Miller, D. D., Callaham, D. A., Shipley, A. M., Rivers, B. A., Cresti, M. & Hepler, P. K. (1994). Pollen tube growth is coupled to the extracellular calcium ion flux and the intracellular calcium gradient: effect of BAPTA-type buffers and hypertonic media. *Plant Cell* **6**, 1815–1828.

Pringle, J. R. (1991). Staining of bud scars and other cell wall chitin with calcofluor. *Methods Enzymol* **194**, 732–735.

Prokisch, H., Yarden, O., Dieminger, M., Tropschug, M. & Barthelmess, I. B. (1997). Impairment of calcineurin function in *Neurospora crassa* reveals its essential role in hyphal growth, morphology and maintenance of the apical Ca^{2+} gradient. *Mol Gen Genet* **256**, 104–114.

Downloaded from www.sgmjournals.org by
IP: 93.91.26.109
On: Wed, 02 Sep 2015 10:32:12

Read, N. D., Kellock, L. J., Knight, H. & Trewavas, A. J. (1992). Contact sensing during infection by fungal pathogens. In *Perspectives in Plant Cell Recognition*, pp. 137–172. Edited by J. A. Callow & J. R. Green. Cambridge: Cambridge University Press.

Robson, G. D., Wiebe, M. G. & Trinci, A. P. J. (1991). Involvement of Ca^{2+} in the regulation of hyphal extension and branching in *Fusarium graminearum* A 3/5. *Exp Mycol* **15**, 263–272.

Sambrook, J., Fritsch, E. F. & Maniatis, T. (1989). *Molecular Cloning: a Laboratory Manual*, 2nd edn. Cold Spring Harbor, NY: Cold Spring Harbor Laboratory.

Schardl, C. L., Panaccione, D. G. & Tudzynski, P. (2006). Ergot alkaloids – biology and molecular biology. *Alkaloids Chem Biol* **63**, 45–86.

Scheffer, J. & Tudzynski, P. (2006). In vitro pathogenicity assay for the ergot fungus *Claviceps purpurea*. *Mycol Res* **110**, 465–470.

Scheffer, J., Ziv, C., Yarden, O. & Tudzynski, P. (2005). The COT1 homologue CPCOT1 regulates polar growth and branching and is essential for pathogenicity in *Claviceps purpurea*. *Fungal Genet Biol* **42**, 107–118.

Schoffelmeer, E. A. M., Klis, F. M., Sietsma, J. H. & Cornelissen, B. J. C. (1999). The cell wall of *Fusarium oxysporum*. *Fungal Genet Biol* **27**, 275–282.

Silverman-Gavrila, L. B. & Lew, R. R. (2002). An IP3-activated Ca^{2+} channel regulates fungal tip growth. *J Cell Sci* **115**, 5013–5025.

Silverman-Gavrila, L. B. & Lew, R. R. (2003). Calcium gradient dependence of *Neurospora crassa* hyphal growth. *Microbiology* **149**, 2475–2485.

Smit, R. & Tudzynski, P. (1992). Efficient transformation of *Claviceps purpurea* using pyrimidine auxotrophic mutants: cloning of the OMP decarboxylase gene. *Mol Gen Genet* **234**, 297–305.

Tasaka, Y., Nakagawa, Y., Sato, C., Mino, M., Uozumi, N., Murata, N., Muto, S. & Iida, H. (2000). *yam8*$^{+}$, a *Schizosaccharomyces pombe* gene, is a potential homologue of the *Saccharomyces cerevisiae MID1* gene encoding a stretch-activated Ca^{2+}-permeable channel. *Biochem Biophys Res Commun* **269**, 265–269.

Tenberge, K. B. (1999). Biology and life strategy of the ergot fungi. VI. Ergot – The Genus *Claviceps*. In *Medicinal & Aromatic Plants – Industrial Profiles*, pp. 25–56. Edited by V. Křen & L. Cvak. Amsterdam & London: Harwood Academic Publishers.

Tenberge, K. B., Homann, V., Oeser, B. & Tudzynski, P. (1996). Structure and expression of two polygalacturonase genes of *Claviceps purpurea* oriented in tandem and cytological evidence for pectinolytic enzyme activity during infection of rye. *Phytopathology* **86**, 1084–1097.

Torralba, S. & Heath, I. B. (2001). Cytoskeletal and Ca^{2+} regulation of hyphal tip growth and initiation. *Curr Top Dev Biol* **51**, 135–187.

Tudzynski, P. & Scheffer, J. (2004). *Claviceps purpurea*: molecular aspects of a unique pathogenic lifestyle. *Mol Plant Pathol* **5**, 377–388.

Watts, H. J., Véry, A. A., Perera, T. H., Davies, J. M. & Gow, N. A. R. (1998). Thigmotropism and stretch-activated channels in the pathogenic fungus *Candida albicans*. *Microbiology* **144**, 689–695.

Yoshimoto, H., Saltsman, K., Gasch, A. P., Li, H. X., Ogawa, N., Botstein, D., Brown, P. O. & Cyert, M. S. (2002). Genome-wide analysis of gene expression regulated by the calcineurin/Crz1p signaling pathway in *Saccharomyces cerevisiae*. *J Biol Chem* **277**, 31079–31088.

Edited by: J. F. Ernst

Downloaded from www.sgmjournals.org by
IP: 93.91.26.109
On: Wed, 02 Sep 2015 10:32:12